GEOPHYSICAL RESEARCH LETTERS, VOL. 31, L05110, doi:10.1029/2003GL018430, 2004

Trajectory studies of large HNO_3-containing PSC particles in the Arctic: Evidence for the role of NAT

K. A. McKinney,[1,2] P. O. Wennberg,[1] S. Dhaniyala,[1,3] D. W. Fahey,[4] M. J. Northway,[4] K. F. Künzi,[5] A. Kleinböhl,[5] M. Sinnhuber,[5] H. Küllmann,[5] H. Bremer,[5] M. J. Mahoney,[6] and T. P. Bui[7]

Received 15 August 2003; revised 9 January 2004; accepted 23 January 2004; published 6 March 2004.

[1] Large (5 to >20 μm diameter) nitric-acid-containing polar stratospheric cloud (PSC) particles were observed in the Arctic stratosphere during the winter of 1999–2000. We use a particle growth and sedimentation model to investigate the environment in which these particles grew and the likely phase of the largest particles. Particle trajectory calculations show that, while simulated nitric acid dihydrate (NAD) particle sizes are significantly smaller than the observed maximum particle sizes, nitric acid trihydrate (NAT) particle trajectories are consistent with the largest observed particle sizes. *INDEX TERMS:* 0305 Atmospheric Composition and Structure: Aerosols and particles (0345, 4801); 0320 Atmospheric Composition and Structure: Cloud physics and chemistry; 0340 Atmospheric Composition and Structure: Middle atmosphere—composition and chemistry. **Citation:** McKinney, K. A., et al. (2004), Trajectory studies of large HNO_3-containing PSC particles in the Arctic: Evidence for the role of NAT, *Geophys. Res. Lett.*, *31*, L05110, doi:10.1029/2003GL018430.

1. Introduction

[2] The existence of polar stratospheric clouds (PSCs) in the high latitude stratosphere in winter is essential for producing the Antarctic ozone hole and the large loss of ozone in some Arctic springtimes [*WMO*, 2002]. Many details of the cloud formation processes and composition remain unresolved, particularly predictive knowledge of PSC particle phases and size distributions in vortex air parcels [*WMO*, 2002]. Identification of the phases is necessary to develop a quantitative understanding of polar ozone loss because particle phase determines the growth and evaporation rates of the particles and therefore the rate of denitrification.

[3] PSC particles larger than several microns in diameter achieve significant fall speeds, resulting in denitrification, i.e., the irreversible redistribution of HNO_3 from higher to lower altitudes [*Fahey et al.*, 1990]. Liquid cloud droplets consisting of supercooled ternary solutions (STS) of H_2SO_4, HNO_3, and H_2O do not affect significant denitrification due to their small sizes [*WMO*, 2002]. However, nucleation of a small number of solid particles with a vapor pressure lower than STS can result in the transfer of a large fraction of the total available nitric acid to just a few particles, which can then grow to sizes large enough for denitrification to occur [*Salawitch et al.*, 1989; *Toon et al.*, 1990]. Solid cloud particles may be composed of $HNO_3 \bullet 3H_2O$ (NAT), the most thermodynamically stable phase under stratospheric conditions [*Hanson and Mauersberger*, 1988], or metastable HNO_3 hydrates, particularly $HNO_3 \bullet 2H_2O$ (NAD), which may nucleate more easily than NAT in the stratosphere [*Worsnop et al.*, 1993].

[4] During the SAGE III Ozone Loss and Validation Experiment (SOLVE) in the winter of 2000, instruments aboard the NASA ER-2 detected low number densities of large (5 to >20 μm) HNO_3-containing cloud particles throughout much of the Arctic vortex [*Fahey et al.*, 2001; *Northway et al.*, 2002a]. This was the first observation of PSC particles large enough to explain extensive vortex-wide denitrification [*Northway et al.*, 2002b]. The large sizes imply that the particles were likely solids, most probably NAT or NAD [*Fahey et al.*, 2001]. For particles of this size to exist at the ER-2 flight altitudes (~20 km), they must have grown for several days prior to the observations [*Fahey et al.*, 2001; *Carslaw et al.*, 2002].

[5] In this study we model the growth and sedimentation of solid particles at and above the ER-2 flight level under various assumptions about their phase. The results show that in January and early February of 2000, the largest particles carrying HNO_3 through the lower stratosphere could not be composed of NAD. In contrast, the observations can be explained adequately if the particles were NAT.

2. Model Description

[6] A standard particle growth model [*Dhaniyala et al.*, 2002] is used to calculate particle size and altitude as a function of time. Changes in ambient pressure (due to particle sedimentation) and temperature (based on air parcel histories) are taken into account. HNO_3 vapor pressures above NAT, NAD, and STS are calculated using relationships derived by *Hanson and Mauersberger* [1988], *Worsnop et al.* [1993], and *Carslaw et al.* [1995]. In all calculations a water vapor mixing ratio of 5 ppmv and a total H_2SO_4 mixing ratio of 0.5 ppbv are used.

[7] Temperature fields (vs. Θ and time) are derived from NMC data using the GSFC trajectory model [*Schoeberl and*

[1]Division of Geological and Planetary Sciences, California Institute of Technology, Pasadena, California, USA.
[2]Now at Department of Chemistry, Amherst College, Amherst, Massachusetts, USA.
[3]Now at Department of Mechanical and Aeronautical Engineering, Clarkson University, Potsdam, New York, USA.
[4]NOAA Aeronomy Laboratory, Boulder, Colorado, USA.
[5]Institute of Environmental Physics, University of Bremen, Bremen, Germany.
[6]Jet Propulsion Laboratory, California Institute of Technology, Pasadena, California, USA.
[7]NASA Ames Research Center, Moffett Field, California, USA.

0094-8276/04/2003GL018430

Sparling, 1994]. 10-day back trajectories (henceforth air parcel histories) were initialized at locations every ~1500 s along the ER-2 flight track at 10 K intervals between 350 and 600 K. Based on a comparison between the GSFC temperatures and those measured by the ER-2 Microwave Temperature Profiler [*Denning et al.*, 1989], we have adjusted the air parcel temperatures by −1.25 K. Divergence of a set of air parcels due to wind shear was neglected for the 4 to 6 day particle trajectories, i.e., the parcels initialized at and above the ER-2 were treated as a column in which a particle resided for its entire history. This approach differs from that used in studies by *Tabazadeh et al.* [2001] and *Drdla et al.* [2003] who obtain vertical temperature profiles at the locations of an isentropic trajectory on one theta level. It also differs from that used by *Fahey et al.* [2001] and *Carslaw et al.* [2002], where particle back trajectories were calculated in a 3-D model.

[8] Altitude profiles of gas-phase HNO_3 were obtained by the ASUR instrument [*von König et al.*, 2000] on three DC-8 deployments spanning December 1999, January and March 2000. For each period, profiles within the polar vortex (using the Nash criterion for the vortex edge [*Nash et al.*, 1996]), were averaged together to obtain a single HNO_3 altitude profile ($1\sigma \leq 25\%$, see supplementary material, Figure 4[1]). For January, a mean profile was also obtained from measurements at positions inside the vortex without PSC coverage to estimate the amount of HNO_3 that would be available without uptake onto PSCs and denitrification, and to serve as a basis for sensitivity studies.

3. Constraints on Particle Growth

[9] Gas-phase HNO_3 never fully equilibrates with the rapidly sedimenting solid particles. As a result, kinetic processes controlling particle growth must be explicitly included to adequately model the growth and sedimentation of these particles.

[10] The presence of liquid STS particles creates a 'growth window' for the solid phases, analogous to the 'nucleation window' described by *Tabazadeh et al.* [2001]. STS droplets take up significant HNO_3 at low temperatures ($T \leq 193$ K), and dominate the total particle surface area. Hence they equilibrate with the gas phase rapidly (~hours), and the vapor pressure over STS limits solid particle growth rates at the lowest temperatures. As a result, the NAT particle growth rate is significant only over a temperature range of about 6 K below the NAT existence temperature (T_{NAT}); NAD growth is limited to an even narrower range. As shown in Figure 1, the NAD growth rates and temperature range are smaller at all altitudes than are those for NAT. Significant denitrification occurred during December and January 2000 [*Popp et al.*, 2001; *Kleinböhl et al.*, 2002], resulting in a decrease in the HNO_3 mixing ratio, and therefore in the temperature range and maximum growth rate.

[11] Above ~26 km, temperatures in the vortex typically increase with altitude, finally making the existence of PSCs impossible. Between January 1 and February 3, 2000, the maximum altitude where nitric acid hydrate particles could form was 30 km. Upper limits on the sizes of particles that can grow in this environment can be calculated by assuming that the particles originate at 28 km and experience the peak growth rate at all altitudes (Figure 1). For the December HNO_3 profile, the maximum particle size at 20 km is ~22.5 μm for NAT and ~19.5 μm for NAD. In January these drop to 20.5 and 17.5, respectively.

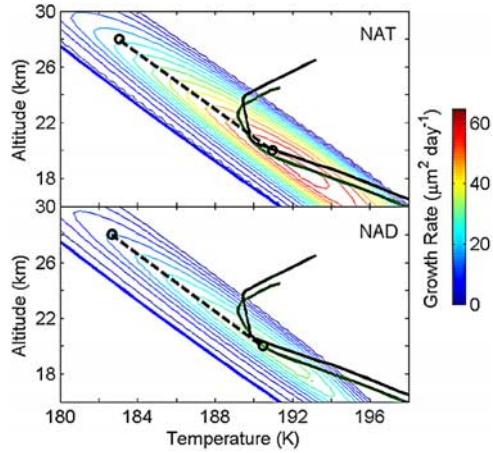

Figure 1. Growth rate (color scale) for a 10 μm NAT (top) or NAD (bottom) particle as a function of temperature and altitude calculated using the January average HNO_3 profile. Also shown are the mean temperature profile obtained by the MTP instrument during the 20 January 2000 ER-2 flight (green line), the mean temperature profile from the air parcel back trajectory data for the same time period (black line), and the ice formation temperature (heavy blue line). The dashed lines show the maximum growth rate vs. altitude.

4. Particle Trajectory Calculations

[12] To test whether the simulated particle sizes are consistent with the SOLVE ER-2 observations, particle diameter and altitude are traced backwards in time (i.e., from a final size and location) by integrating the growth and sedimentation equations and accounting for changing stratospheric conditions as described in Section 2. For each ER-2 flight segment, the back trajectories of 2 to 26 μm diameter particles were calculated assuming either NAT or NAD composition.

[13] Figure 2 shows an example of particle trajectories for one segment of the 31 January 2000 flight. Two types of trajectories are observed. In a "successful" trajectory, the particle remains below the NAT (NAD) existence temperature during most of its history, and can be traced from its final size and position to the point at which its diameter was near zero. "Unsuccessful" trajectories, on the other hand, spend insufficient time in the growth window and cannot be traced to an origin. These trajectories generally require that the particles be unrealistically large (>40 μm) at some time, or that they enter the model domain (32 km) already at significant size – clearly unrealistic as temperatures above this altitude are too warm for PSCs.

[14] Typically, all trajectories up to a certain maximum size are successful because particles smaller than the maximum require shorter growth times and/or less cold temperatures. Thus, for each flight segment and phase we can estimate the maximum particle size. The maximum

[1]Auxiliary material is available at ftp://ftp.agu.org/apend/gl/2003GL018430.

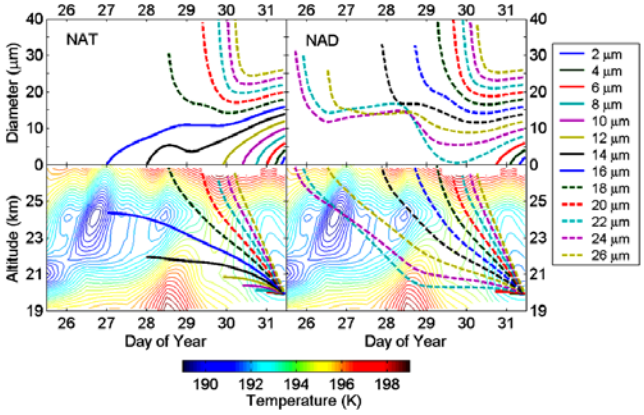

Figure 2. Particle back trajectories for NAT (left) and NAD (right) particles originating at the altitude of the ER-2 between 39040 and 40500 UTS on 31 January 2000. The temperature fields derived from isentropic air parcel histories are shown in color scale. Trajectories for final particle sizes of 2–26 μm are shown. Solid lines denote successful and dashed lines unsuccessful trajectories. NAT particles up to 16 μm and NAD particles up to 6 μm in diameter are predicted for these conditions.

NAT particle size is always larger than the maximum NAD particle size. In the case shown in Figure 2, where particles with a maximum size between 16 and 21 μm were observed, NAT particles up to 16 μm could have been present, whereas NAD particles of only 6 μm diameter are achievable.

5. Comparison With Observations

[15] During SOLVE, three instruments on the NASA ER-2 detected large HNO_3-containing particles between 16 and 21 km in the Arctic vortex. The NOAA Aeronomy Laboratory NOy instrument front inlet channel detected individual large particles as short duration pulses of NOy [*Fahey et al.*, 2001; *Northway et al.*, 2002a]. The integrated amount of NOy in each pulse, minus the amount in the gas phase and small particles as measured in the rear channel, can be related to the mass, and therefore diameter, of the evaporated particle (assuming spherical particles of a known density and phase) [*Northway et al.*, 2002a]. Similarly, the Caltech Chemical Ionization Mass Spectrometer (CIMS) detected short HNO_3 pulses after evaporation of these large particles in its inlet, verifying that the NOy content of the large particles was indeed nitric acid. The ER-2 MASP instrument also measured the number size distributions of the large particles [*Brooks et al.*, 2003].

[16] Large nitric acid containing particles were detected over significant portions of the flights of 20 and 31 January and 3 February 2000. We estimate the sizes of the largest particles observed in each flight segment using an NOy data analysis approach similar to that described in *Northway et al.* [2002a] and compare the observed maximum sizes to those predicted by the back trajectory calculations described in Section 4.

[17] The maximum particle sizes derived from the data are shown with those from the trajectory calculations in Figure 3. The January HNO_3 profile, believed to be representative of the conditions in the Arctic vortex during the observation period, is used in the base cases. Simulations were also performed using the HNO_3 profile obtained from locations without PSCs as an upper limit, and the vortex-average January profile −25% as a lower limit. These profiles range from ∼5.5 to 10.5 ppbv at the peak of the HNO_3 profile near 20 km. Maximum size calculations were performed for the base temperature ±1.5 K, typically resulting in differences in particle size of <2 μm. In some cases, the calculated maximum size actually decreases with decreasing temperature, as uptake on STS limits gas phase HNO_3. Uncertainties in the measured vapor pressures (∼20%) [*Hanson and Mauersberger*, 1988; *Worsnop et al.*, 1993; *Carslaw et al.*, 1995] result in differences in the maximum calculated diameters of 1–2 μm (not included in the figure.)

[18] To test the validity of the temperature fields derived using the air parcel column assumption, particle back trajectories were calculated stepwise in one day intervals for selected flight segments (i.e., using initial air parcel

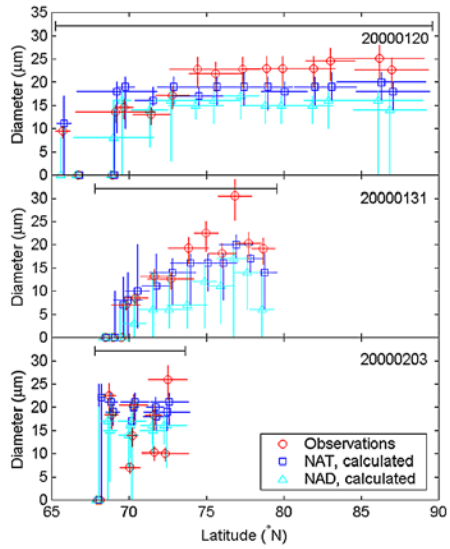

Figure 3. Comparison of observed (red) and calculated maximum particle sizes assuming NAT (blue) and NAD (cyan) for three ER-2 flights. The black bar shows the latitude range covered in each flight. Data is binned vs. time; the horizontal bars represent the range of latitudes sampled during each time bin. For the simulations, the January HNO_3 profile is used to determine the most likely maximum particle size (markers). The vertical bars represent the range in maximum particle sizes under the various total HNO_3 and temperature conditions discussed in the text. For the observations, the vertical bars represent the range in possible maximum particle mass obtained by calculating the net NOy signal due to particles >2 μm and correcting the particle signal heights using the average response function described in *Northway et al.* [2002a] to find an upper limit for the maximum particle size. To estimate a lower limit, we assume that due to sampling of multiple particles in a single time bin, the mass of the largest particles could be a factor of 2 lower than the upper limit. The diameter range shown includes the difference in particle sizes determined assuming NAT (upper limit) or NAD (lower limit) particle composition, which differ by ∼10%.

histories, one day particle trajectories were calculated, then new air parcel histories were calculated from the new particle location, and this process was iterated for the lifetime of the particle.) The resulting maximum particle sizes were always within the range of sizes determined using the column assumption and ±1.5 K temperature uncertainty.

[19] At latitudes polewards of 73°N, the calculated maximum NAT particle sizes are similar to the observed maximum particle sizes. In contrast, the calculated NAD particle sizes are smaller than those observed. At the edge of the vortex, where temperatures are near the NAT existence temperature and air parcel histories are less certain, the predicted maximum size ranges for NAD do sometimes overlap the observed maximum particle sizes. Hence we can differentiate between the phases with less certainty. Even so, the maximum sizes are better reproduced by assuming NAT rather than NAD, particularly on 20000131.

6. Discussion and Conclusions

[20] These results indicate that unless the largest particles are composed of a crystalline phase not considered here, they most likely either nucleated as NAT, or if they nucleated as NAD, they likely converted to NAT shortly after nucleation. We calculate that for a particle to grow to 20 μm at 20 km, it must have been NAT for at least the last 2 days of its 6–7 day trajectory. This analysis provides some of the strongest evidence to date for the existence of NAT among the large, denitrifying PSC particles observed in the Arctic during SOLVE. The remainder of the particles in the large mode experienced conditions similar to the largest particles, suggesting that all the particles in this mode may be composed of NAT. Assuming a realistic size distribution (D = 14.5 μm, σ = 2.45 see *Fahey et al.* [2001]), particles ≥18 μm (i.e., NAT particles) account for 25% of the total HNO_3 flux.

[21] In other recent studies *Carslaw et al.* [2002] calculated particle forward trajectories in a 3-D model and compared the resulting NAT and NAD size distributions to the observations. Because the size distributions overlap one another substantially, they could not exclude NAD. In their study, HNO_3 uptake on STS was not explicitly included. Here we are able to differentiate between the two phases by including STS and focusing only on the largest particles. *Drdla et al.* [2003] used a column model along trajectories to trace PSC evolution, comparing the results with observed PSC extent, denitrification, and dehydration. They concluded that, although they could not rule out NAD, the NAT simulations agreed more favorably with the measurements. Our conclusions are consistent with these earlier studies.

[22] For large particles to be present, solid particle nucleation (by an undetermined mechanism) must occur at the start of the trajectory. The simulations presented here are independent of the nucleation mechanism. Hence, it is possible to find conditions under which the growth of large particles is predicted, but none are observed because nucleation did not occur. It is therefore interesting to note that for almost all intervals during these flights when the calculated trajectories were successful large particles were also observed.

[23] **Acknowledgments.** Thanks to Drs. L. Lait, M. Schoeberl, and P. A. Newman of the Atmospheric Chemistry and Dynamics branch at NASA GSFC for use of the Goddard Automailer. This work was supported by NSF Grant No. ATM9871353 and NASA Grant No. NAG5-8922. Work at JPL, California Institute of Technology, was carried out under contract with NASA.

References

Brooks, S. D., et al. (2003), Measurements of large stratospheric particles in the Arctic polar vortex, *J. Geophys. Res.*, *108*(D20), 4652, doi:10.1029/2002JD003278.

Carslaw, K. S., et al. (1995), An analytic expression for the composition of aqueous HNO_3 – H_2SO_4 stratospheric aerosols including gas phase removal of HNO_3, *Geophys. Res. Lett.*, *22*(14), 1877–1880.

Carslaw, K. S., et al. (2002), A vortex-scale simulation of the growth and sedimentation of large nitric acid hydrate particles, *J. Geophys. Res.*, *107*(D20), 8300, doi:10.1029/2001JD000467.

Denning, R. F., et al. (1989), Instrument description of the airborne microwave temperature profiler, *J. Geophys. Res.*, *94*, 16,757–16,765.

Dhaniyala, S., et al. (2002), Lee-wave clouds and denitrification in the polar stratosphere, *Geophys. Res. Lett.*, *29*(9), doi:10.1029/2001GL013900.

Drdla, K., et al. (2003), Microphysical modeling of the 1999–2000 Arctic winter: 1. Polar stratospheric clouds, denitrification, and dehydration, *J. Geophys. Res.*, *108*(D5), 8312, doi:10.1029/2001JD000782.

Fahey, D. W., et al. (1990), Observations of denitrification and dehydration in the winter polar stratospheres, *Nature*, *344*, 321–324.

Fahey, D. W., et al. (2001), The detection of large HNO_3-containing particles in the winter Arctic stratosphere, *Science*, *291*, 1026–1031.

Hanson, D., and K. Mauersberger (1988), Laboratory studies of the nitric acid trihydrate: Implications for the south polar stratosphere, *Geophys. Res. Lett.*, *15*(8), 855–858.

Kleinböhl, A., et al. (2002), Vortexwide denitrification of the Arctic polar stratosphere in winter 999/000 determined by remote observations, *J. Geophys. Res.*, *108*, 8305, doi:10.1029/2001JD001042.

Nash, E. R., et al. (1996), An objective determination of the polar vortex using Ertel's potential vorticity, *J. Geophys. Res.*, *101*(D5), 9471–9478.

Northway, M. J., et al. (2002a), An analysis of large HNO_3-containing particles sampled in the Arctic stratosphere during the winter of 1999/2000, *J. Geophys. Res.*, *107*(D20), 8289, doi:10.1029/2001JD001079.

Northway, M. J., et al. (2002b), Relating inferred NOy flux values to the denitrification of the 1999–2000 Arctic vortex, *Geophys. Res. Lett.*, *29*(16), 1816, doi:10.1029/2002GL015000.

Popp, P. J., et al. (2001), Severe and extensive denitrification in the 1999–2000 Arctic winter stratosphere, *Geophys. Res. Lett.*, *28*(15), 2875–2878.

Salawitch, R. J., et al. (1989), Denitrification in the Antarctic stratosphere, *Nature*, *339*, 525–527.

Schoeberl, M. R., and L. C. Sparling (1994), "Trajectory Modelling"; Diagnostic Tools in Atmospheric Physics, Proc. S. I. F. Course CXVI, edited by G. Fiocco and G. Visconti, North-Holland, Amsterdam.

Tabazadeh, A., et al. (2001), Role of the stratospheric polar freezing belt in denitrification, *Science*, *291*, 2591–2594.

Toon, O. B., et al. (1990), Denitrification mechanisms in the polar stratospheres, *Geophys. Res. Lett.*, *17*(4), 445–448.

von König, M., et al. (2000), An airborne sub-mm radiometer for the observation of stratospheric trace gases, in Microw. Radiomet. Remote Sens. Earth's Surf. Atmosphere, edited by P. Pampaloni and S. Paloscia, 409–415.

WMO (2002), Scientific assessment of ozone depletion: 2002 (Rep. 47), World Meteorological Organization, Geneva, Switzerland.

Worsnop, D. R., et al. (1993), Vapor pressures of solid hydrates of nitric acid: Implications for polar stratospheric clouds, *Science*, *259*, 71–74.

H. Bremer, A. Kleinböhl, H. Küllmann, K. F. Künzi, and M. Sinnhuber, Institute of Environmental Physics, University of Bremen, Bremen, Germany.

T. P. Bui, NASA Ames Research Center, Moffett Field, CA, USA.

S. Dhaniyala, Department of Mechanical and Aeronautical Engineering, Clarkson University, Potsdam, NY, USA.

D. W. Fahey and M. J. Northway, NOAA Aeronomy Laboratory, Boulder, CO, USA.

M. J. Mahoney, Jet Propulsion Laboratory, California Institute of Technology, Pasadena, CA, USA.

K. A. McKinney, Department of Chemistry, Amherst College, Amherst, MA, USA.

P. O. Wennberg, Division of Geological and Planetary Sciences, California Institute of Technology, Pasadena, CA, USA.